Determination of the Intra Uterine Pressure with electrodes on the abdomen

Paul Aelen

December 5, 2005

Abstract

A new method is proposed to determine the intra uterine pressure (IUP) of women during pregnancy.

The IUP is determined out of 3 electrodes on the abdomen of the women and 1 reference electrode on the ankle. The uterine electromyogram (EMG or EHG) is filtered out of a mixture of signals (EHG, Mother and Child ECG, noise). From the bipolar leads of this EHG time frequency representations are made (spectrogram and Wigner Ville) whereafter a feature is extracted with characteristics of power and instantaneous frequency. To match the real IUP, the offset, gain and saturation are calculated between the real and estimates signal. This is done by multiple regression.

Additional information about the propagation direction and velocity of the contractions can be obtained by measuring with more electrodes which might give information about contraction effectiveness and muscle fatigue. The direction and propagation are determined by taking the gradient of the delays of the electrodes. The delays are calculated by crosscorrelating the electrode signals with a reference delay (e.g. the invasive IUP).

The algorithm gives very promising results. Correlations of over 90% are obtained, which makes this algorithm a noninvasive and accurate method. Therefor it is a better tool than tocography and invasive measurements for measuring IUP.

Contents

Introduction

Fetal monitoring has become a very important tool, to control a fetuses health. Especially at labour, when the fetus is confronted with hypoxia (a lack of oxygen) monitoring is of vital importance. In order to come through labor well, the fetus is equipped with protective mechanisms which enable it to cope with significant oxygen deficiency. When these mechanisms aren't able to react properly to hypoxia, permanent damage to the fetus can be risked. Monitoring the health of the fetus has thus become very important for gynaecologists to see if there are situations that must be prevented.

The main protective mechanism that can be measured noninvasive is the fetal heart rate. When a fetus is stressed, the heart rate increases. As uterine contractions can impose stress on the fetus, the relation between these variables provides information on the condition of the fetus.

Monitoring of the fetuses heart rate and the mother's uterine contractions during pregnancy and labour is nowadays mostly done by external tocography (TOCO), a simple and noninvasive measurement technique. Contractions are recorded by a tensometric transducer, which is attached to the mothers abdomen. The problem with this method is its limited accuracy and sensitivity. Another technique is the direct measurement of intra uterine pressure. This is done by directly recording the pressure in the uterus with a pressure transducer. The limitation of this method is the invasive aspect,it can harm the fetus and the mother. A second problem is that this kind of measurement only can preformed when the mother's membranes are ruptured, thus only at labour. A new method should have the advantages of the two, it should be noninvasive and the accuracy and sensitivity should be high. A method which could have those advantages could be electrohysterography (EHG). It consists in recording of action potentials of myometrium cells by means of electrodes positioned at the women's abdomen. Besides information on the condition of the fetus the electrohysterogram can also provide information about fetus motion, early detection of premature labour /term prediction and uterine activity knowledge.

The ultimate goal of this project is the determination of the intra uterine pressure (IUP) with electrodes on the abdomen of the women. In this report an algorithm is developed which implements this idea with EHG measurements.

The report starts in chapter 1 with the physiology and the electrical activity of the uterus. Chapter 2 gives information about the data acquisition and the signals that are present at the abdomen of the mother. Chapter 3 handles with the preprocessing of the signal and the determination of the IUP out of the electrode signals. Finally chapter 4 presents and discusses the results that are obtained.

Chapter 1

The Uterus

1.1 Physiology

The uterus is the major female reproductive organ. It mostly consists of muscular fiber, which forms a thick wall around a hollow space. It's size and shape are roughly that of an upside down pear. The uterus is located in the pelvis cavity immediately dorsal to the urinary bladder and ventral to the rectum. Normally, the diameter of the uterus is several centimeters, but during pregnancy it grows enormously.The wall of the uterus consists of three layers, the endometrium, myometrium and serosa.

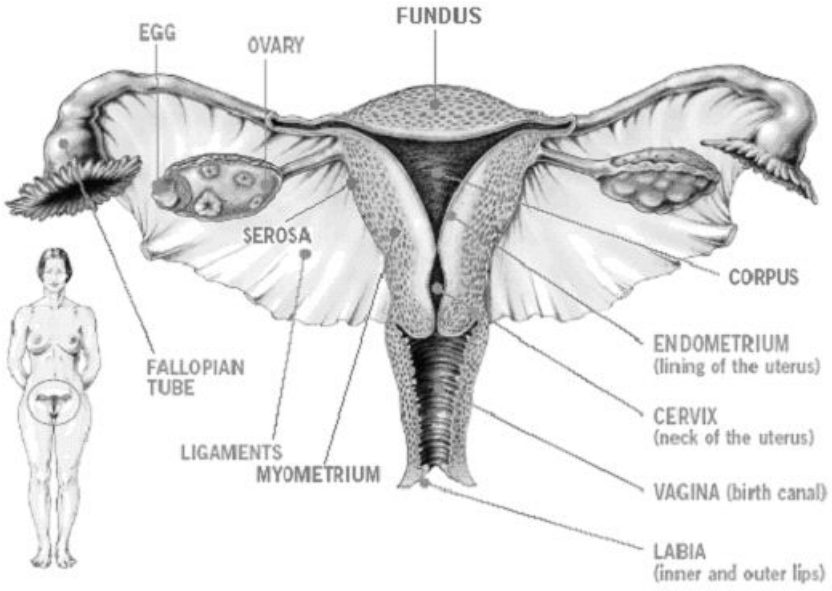

Figure 1.1: Anatomy of the uterus

The endometrium is the uterine innermost membrane which thickens in preparation for the implantation of a fertilized egg upon its arrival into the uterus. It is rich in blood vessels, which are connected to by the new embryo, forming a placenta through which the embryo, as it becomes a fetus and eventually gestates fully, receives oxygen and is nourished. In absence of implantation some part of the endometrial lining sheds. This is called menstrual bleeding. The whole cycle of thickening and shedding is 28 days long in average.

The middle and thickest layer of the uterus is called the myometrium. It consists of smooth involuntary muscle and supporting stromal and vascular tissue. During pregnancy the myometrium stretches by means of hypertrophy (the muscle cells expand in size, rather than number). When

parturition takes place the myometrium contracts in a coordinated fashion to propel the fetus out of the uterus. After delivery the myometrium contracts to expel the placenta and reduce blood loss. After pregnancy the uterus returns to its nonpregnant size by a process of myometrial involution. During menstruation, the myometrium contracts at little amounts to help expel the endometrium lining.

The serosa (or visceral peritoneum) is the outermost layer of the uterus. This layer is a part of the peritoneum, a multilayered membrane which lines the abdominal cavity, and supports and covers the organs within it. The outer part of the peritoneum that lines the abdominal cavity is called the parietal peritoneum. The portion that covers the uterus (and also other organs), is known as the visceral peritoneum and forms the outer layer (serosa) of most of the intestinal tract.

The hollow empty space that is mentioned before is called the corpus. It is the main part of the uterus, which grows during pregnancy and carries the fetus. At the lower end the corpus narrows and forms the cervix, which is the narrow cylindrical passage to the uterus which connects to the vagina. The vagina, or the "birth canal" is a muscular tube which extends from the opening of the uterus to the outside world.

At either side of the cranial end of the uterus a Fallopian tube is attached, which is a delicate muscular tube. Each fallopian tube terminates at or near an ovary. When an egg is released from an ovary, it travels trough the tube to the uterus. When the egg is fertilized it implants itself in the uterine lining and retains there till birth.

1.2 Excitation and contraction

The mechanical contractions of the uterus depend on the excitation and propagation of electrical activity. When the resting potential of a cell (the potential difference between the negative inside and positive outside of the cell) depolarizes (becomes more positive) and eventually reaches a certain threshold, one or a burst of action potentials is generated. An action potential is an irreversible sudden change in membrane potential, where this potential difference even can become positive. Because the resting potential of uterine smooth muscle cells fluctuate in a random way, AP's are generated spontaneously by an occasionally exceeding of the threshold.

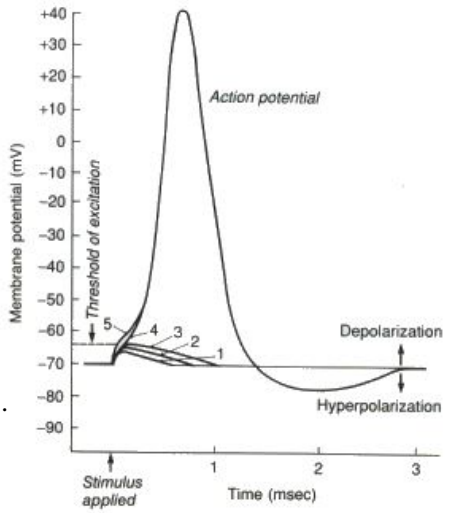

Figure 1.2: An Action Potential

The startingpoint of AP's is called the pacemaker(area). Because of the randomness of the fluctuations the place of the pacemaker varies in time.

After an AP is generated the muscle cell has to retain its resting potential. This is called repolarisation. In this time it is more difficult or even impossible to generate a new action potential. The period where the membrane is less sensitive is called the refractory period. Action potentials are propagated by gap junctions. These are intercellular channels that link cells to their neighbors, allowing passage of some inorganic ions and small molecules. They appear in areas of close apposition between cells as zones of paired parallel membranes, of unusually smooth outline, separated by a narrow space of constant width, the gap. When the propagated AP's reach a refractory area, they seize up and extinguish. The conduction speed of action potentials through the myometrial muscle is relatively small, limiting the frequency content from 0 to 3 Hz. As pregnancy progresses the frequency spectrum is shifted somewhat to higher frequency's because of the increasing number of gap junctions. The maximum frequency is however never higher than 5 Hz.

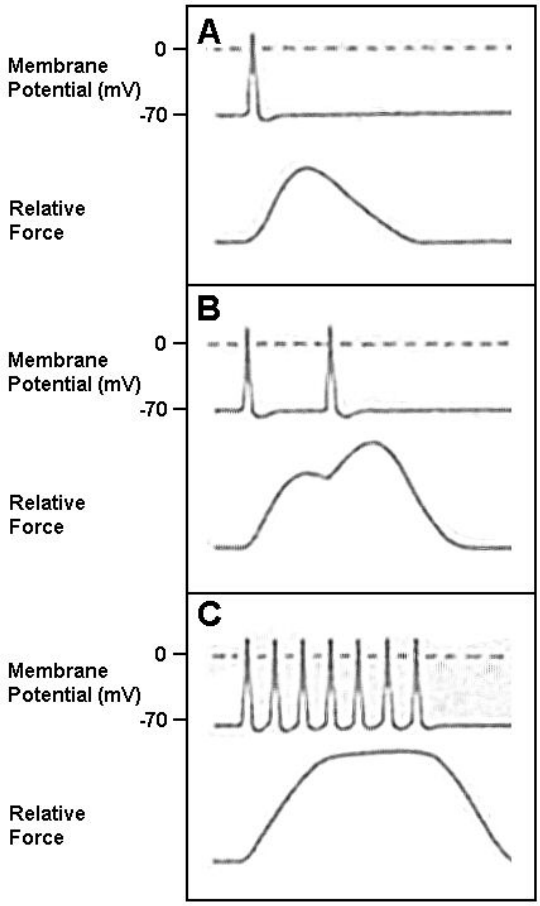

Figure 1.3: (a) A single twitch, (b) Spatial summation (c) Tetanic contraction

Uterine smooth muscle cells contain thin actin and thick myosin filaments, like striated muscles. The contractile mechanism involves the interaction of these two specific protein filaments. The excitation-contraction coupling is mediated by calcium-ion fluxes. The intracellular Ca2+ concentration is very low when the muscle is at rest. When an action potential arrives, this concentration increases, which in turn, controls the interaction between the contractile proteins. The mechanical reaction to an AP is a single twitch of several milliseconds. When a burst of AP's arrives, the single twitches overlap and form a smooth contraction. When the frequency of AP's increases, the contractile strength becomes higher.

Sex steroids influence the excitation and propagation of AP's; e.g. it is supposed that at parturition the propagation of a contraction is initiated at the junction of the fallopian tube and the uterus on one side and propagates in descending direction along the uterus. This indicates a fixed pacemaker area which isn't the case in the beginning of labour. The influence of sex steroids is also seen in the different kind of contractions that encounter during pregnancy: During the first 30 weeks of pregnancy, the uterus exhibits very low-amplitude contractions at a frequency of approximately one per minute, the Alvarez waves. From the twentieth week of gestation, the so-called Braxton-Hicks contractions appear. These contractions have higher amplitude and occur every 3 to 4 hours. As pregnancy progresses, these contractions become more and more frequent and increase in strength. At parturition activity is considered to be fully "propagated" through the whole uterus in a short time (about 20 sec) [Dev93]. A third influence of sex steroids is seen in the propagation of action potentials. The number of gap junctions increases greatly, allowing faster propagation of action potentials and increasing the coordination of contractility.

1.3 Electromyography (EMG)

The recording of the propagating action potentials is called the uterine electromyogram (EMG) or electrohysterogram (EHG). The recording provides information about contractions in obstetric monitoring. Because the strength of a contraction depends on the frequency of arriving AP's, a higher frequency in the EHG represents an stronger contraction. In electrical engineering this is known as frequency modulation (FM). By demodulating the EHG signal, the shape of the contractions could be made visible [Man92]. Because of the use of surface-electrodes (see chap 2) there is spatial summation of AP's from different origin's. The EHG signal is thus an summation of frequency modulated signal. This EHG can be measured invasively directly at the myometrium or on the abdomen. EHG's recorded by surface electrodes on the abdomen represent the spatial summation of cellular activity. This spatial integration implies an increase in signal amplitude and is usually associated with a low pass filtering effect by the conductive properties of the tissue between the uterus and the electrodes.

Describing electromyograms, many authors have made a distinction between two types of waves: a slow wave, with a period equal to the contraction duration and a fast wave superimposed on the slow wave. The slow wave is associated with skin stretching and has no further electrical source. The fast wave contains the information about the muscle activity. The fast wave can be split further in a low (FW_L) and high (FW_H) frequency band. FW_L is associated with frequency's present in every uterine electrical recording and FW_H which is supposed to be related to efficient labour contractions (see figure 1.4).

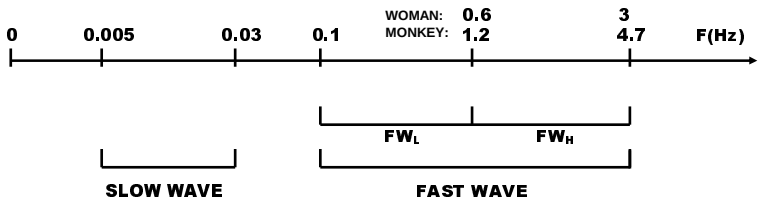

Figure 1.4: Characteristics of EHG frequency content

1.4 IUP Propagation

During pregnancy the propagation of contractions through the uterus become more and more deterministic. The propagation direction of Braxton-Hicks contractions is known to be random while effective contractions are supposed to have an direction from the top of the uterus to the bottom, to perform a pushing action. A visualization of the propagation direction could make a distinction between effective and ineffective contractions, making it a tool that can indicate preterm birth.

The speed of propagation (conduction speed) can give information about the reaction of the muscle to the action potentials that arrive. When a muscle isn't able to contract at the strength that the electrical signal indicates (which is known as muscle fatigue), this is seen in a lower conduction speed [Man05]. For gynaecologists this can be useful for indicating whether nonprogressive labour is due to exhausted muscles or has another source.

Chapter 2

Data Acquisition

The measurements that are performed, are done simultaneously with a pressure transducer and electrodes on the abdomen of the woman. The main goal is to obtain the pressure from these electrode signals, where the signal that is obtained from the pressure transducer is treated as golden standard. All measurements are amplified by the M-PAQ amplifier whereafter they are digitized.

2.1 Pressure Transducer

The pressure transducer that is used to measure the intra uterine pressure is a Koala M1333A from Philips. This device measures the IUP against a reference pressure (e.g. the air pressure), making it a differential measurement. With this device it is only possible making good differential measurements, not absolute pressures. Therefor the offset that is measured with this device isn't reliable, and is not taken into account in the golden standard.

2.2 Electrodes

To explain some properties of measurements with electrodes, an electrode measurement can be modeled by a metal in a solution, the electrolyte. Due to thermal excitation metallic ions leave the metallic lattice and spread through the solution, causing the electrolyte to obtain a positive potential with respect to the electrode. The electrical field that builds up in this way, forces the ions to return to the electrode. Eventually, a dynamic equilibrium is set between the electrical force and thermal excitation, the electrode bias. This bias is in principle not measurable. This is because another electrode is needed which also has such a bias. Only the bias difference between two electrodes can be measured. This potential difference is in the order of 1 V, which in contrast with biomedical signals (order $\mu V \ldots mV$) is very high. This means that the D.C. component of the measured signals should be excluded from amplification. As a result from the electrode bias, the metal ions stay close to the electrode, forming a so-called double layer, which can be modeled as a electrical capacitor. The existence of this double layer is accompanied by two specific problems: motion artifacts and polarization. Ions in the double layer can move freely through the electrolyte, however at limited speeds. When the electrode is moved with respect to the electrolyte, the double layer remains behind, resulting in a momentary fluctuation in the electrode-bias. This fluctuation is represented as a source of noise in the signal. The magnitude of this noise depends strongly on the electrode material. As a current passes through the electrode-electrolyte transition, the double layer is disturbed, again causing a momentary fluctuation in the electrode-bias. This fluctuation is called polarization and its magnitude depends on the frequency of the current, the current density in the transition, the electrode material and the concentration of ions in the electrolyte. In order to minimize the effect of polarization, the current density through the electrode should be kept small. This can be done by the use of a badly insoluble elektrode metal, the use

of electrodes with a large area and the use of a high input impedance amplifier. The electrodes, used for performing the measurements, are Ag/AgCl electrodes. These are Ag electrodes with a thin layer of AcGl, which forms a poreus layer. Because the AgCl dissolves very badly in water, the electrolyte is saturated quickly. The Ag+ concentration near the electrode is now complete constant, which makes this electrode very insensitive to polarization and electrode motion [Clu98].

2.3 Amplifier

The amplifier that is used is the Maastricht-Programmable AcQuisitionsystem (M-PAQ). It is a medical safe universal amplifier system. The system can be used to measure physiological signals (ExG, blood pressure etc.) as well as non-physiological signals (acceleration, force etc.). The analog inputs are digitized inside the amplifier system with a resolution of 20 bits at a sample rate of 500 Hz, which is far below the system's limit of 25 kHz. Further the amplifier has build in filters that for example can filter out the power line interference.

2.4 Electrode Configuration

Because there is no specific pacemaker area during the greatest part of labour, electrodes can be placed anywhere, provided that there are sufficient muscle fibers. The first electrode configuration is in such way that as much of the uterus is covered. When labour progresses, contractions are supposed to propagated in a descending way. For this reason a second electrode configuration is figured out where the electrodes are placed on the vertical median line of the abdomen. This configuration gives a better Signal to Noise Ratio (SNR) because of a closer contact and a more constant position of the uterus to the abdominal wall.

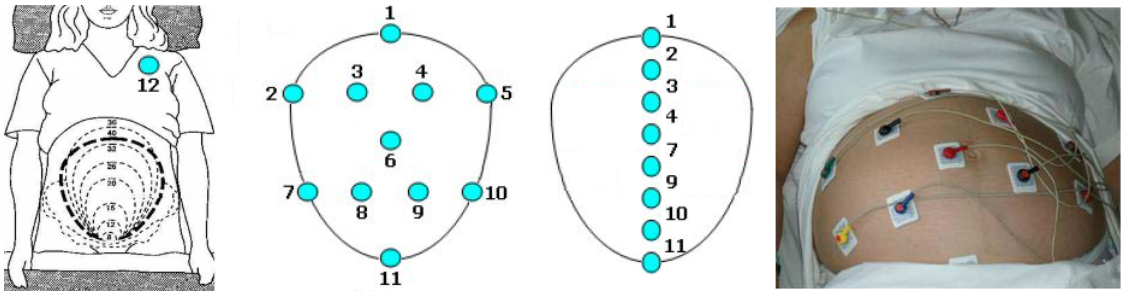

Figure 2.1: From left to right: The mother ECG, whole uterus coverage, median line, a real measurement

The reference for all electrodes is on the right ankle, a place were no signal of the active electrodes is picked up. One extra electrode is placed on the left shoulder of the mother to measure her electrocardiogram (ECG). This is done because the ECG is likely to be prominently present in the abdomen recording because of its relatively large amplitude. When this ECG is measured separately it could be adaptively subtracted from the recordings on the abdomen. All recordings are done with unipolar recordings. The measurements are digitally made bipolar by subtracting electrodes that are close to each other. The advantage of using bipolar leads, is the better SNR it provides, because common noise sources are filtered out by the subtraction.

2.5 Signals

The signal that is measured is a mixture of different sources, the EHG, the ECG of the mother, the ECG of the fetus, power line interference and other kinds of noise. In figures 2.2, till 2.4 the characteristics of these signals are plotted in time and frequency.

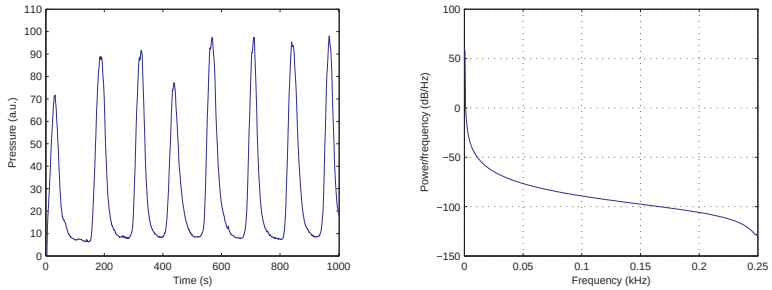

Figure 2.2: left: Typical IUP signal. right: Power spectrum density (PSD) of the IUP

Figure 2.2 shows that the IUP is a very low frequent signal. The content of abdomen EMG is fully captured by frequency's till 5 Hz (chapter 1.2).

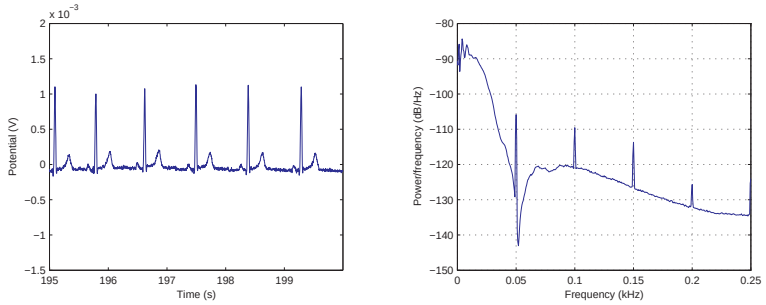

Figure 2.3: left: Typical ECG signal. right: Power spectrum density (PSD) of the ECG

The main source of interference is the ECG of the mother. The main part of this source has a low frequent character (see figure 2.3). A part of the spectrum might overlap the spectrum of the EHG. Further power line interference is superimposed on the ECG, which is seen by the peak at 50 Hz. The peaks at multiples of 50 Hz are caused by the higher harmonics of the power line. Other sources of interference are the ECG of the fetus and motion artifacts of the mother and fetus. The ECG of the fetus has the same characteristics as the mother ECG but at a much lower amplitude. Motion artifacts of the baby and mother have a low frequent content which overlap the spectrum of the EHG. By making the recordings bipolar(see chapter 3.1.1) most of the common noise like mother ECG and motion artifacts can be removed.

In the bipolar EHG signal a contraction of the uterus can be seen by a burst. This can't be seen in the unipolar recording (see figure 2.4). Again the power line interference introduces a high peak at 50 Hz and it's higher harmonics. In the next chapter the EHG is extracted out of the mixture of signals.

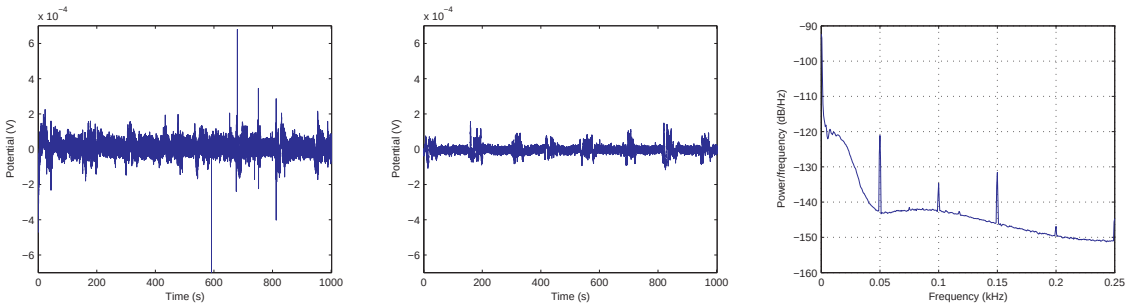

Figure 2.4: left: Raw EHG signal (unipolar). middle: Raw EHG signal (bipolar). right: Power spectrum density (PSD) of the raw signal (bipolar)

Chapter 3

Signal Processing

In this chapter all of the processing is done. First of all, the different electrode signals are preprocessed to extract the EHG signal out of the mixture of signals. Hereafter the EHG is processed to estimate the IUP. This estimate is then fit to the real IUP by multiple regression where parameters are extracted that model the offset, gain and saturation of the electrode signals. In figure an overview of the developed algorithm is shown. The a-value that is subtracted is the offset calculated in the multiple regression. Because the DC value of the electrical signal is more reliable then the pressure signal (chapter 1.4) this value isn't taken into account when evaluating the results.

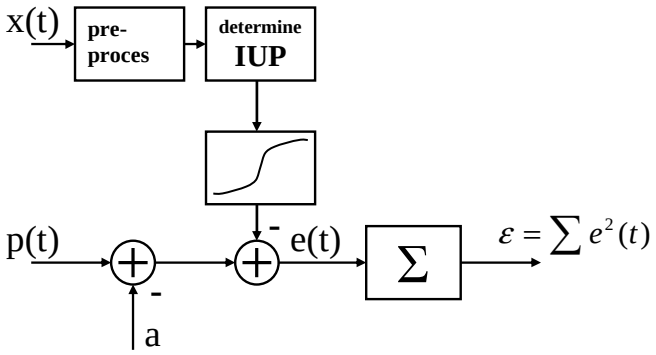

Figure 3.1: Overview of the algorithm

3.1 Preprocessing

3.1.1 Bipolarizing the data

The recordings are made bipolar by subtracting two unipolar recordings that are close to each other. In this way common noise is suppressed, providing a better SNR.

3.1.2 Remove the mother ECG

The mother ECG can be removed by means of an adaptive filter. The ECG of the mother that is measured on the shoulder of the mother is delayed and scaled whereafter it is subtracted from the abdomen signal. The scaling factor and delay vary during the measurement making the subtraction

adaptive. The transfer function of the abdomen is characterized by a FIR filter W, which outcome $\widehat{e}$ is:

$$\widehat{e}[k] = \sum_{i=0}^{N-1} w_i x[k-i] = \underline{x}^t[k]\underline{w} = \underline{w}^t\underline{x}[k] \tag{3.1}$$

The fault r between the real transfer and estimates transfer is:

$$r[k] = e[k] - \widehat{e}[k] \tag{3.2}$$

Optimal values for W can be found by:

$$\underline{w}_{opt} = \min_{\underline{w}} E\{r^2[k]\} \tag{3.3}$$

$$J = E\{r^2[k]\} = \sigma_e^2 - 2\underline{w}^t\underline{\rho}_{ex} + \underline{w}^t R\underline{w} \tag{3.4}$$

$$\frac{\partial J}{\partial \underline{w}} = 2R\underline{w} - 2\underline{\rho} = 0 \qquad \Rightarrow \qquad \underline{w}_{opt} = R^{-1}\underline{\rho} \tag{3.5}$$

The error function J is quadratic in the weight coefficients w_i. For this reason, the steepest descent update for w is taken:

$$\underline{w} = \underline{w} - \alpha\underline{\nabla} \tag{3.6}$$

$$\underline{\nabla}[k] = \Big(\frac{\partial J[k]}{\partial w_0}, \ldots, \frac{\partial J[k]}{\partial w_{N-1}}\Big) = -2E\{\underline{x}[k]rk\} \tag{3.7}$$

The average operation is simplified by the Least Mean Square (LMS) strategy:

$$E\{.\} \qquad \Rightarrow \qquad \underline{\nabla}_{LMS}[k] = -2\underline{x}[k]r[k] \tag{3.8}$$

$$\underline{w}[k+1] = \underline{w}[k] + 2\alpha\underline{x}[k]r[k] \tag{3.9}$$

To make the update of w independent of input statistics and make the parabolic error function symmetric, the update operator $\underline{\nabla}$ is whitened by multiplying it with the inverse autocorrelation matrix R^{-1}.

$$\underline{w}[k+1] = \underline{w}[k] + 2\alpha R^{-1}\underline{x}[k]r[k] \tag{3.10}$$

To speed up the calculations, block processing is used; the output of L samples is calculated per iteration in stead of 1 sample per iteration.

$$\Big(\underline{\nabla}_{BLMS}[kL]\Big)_i = \frac{-2}{L}\sum_{q=0}^{L-1} x[kL-i-q]r[kL-q] \tag{3.11}$$

$$\underline{w}[(k+1)L] = \underline{w}[kL] + \frac{2\alpha}{L}R^{-1}x[kL]\underline{r}[kL] \tag{3.12}$$

All the processing is done in frequency domain to make the algorithm more efficient arriving at an Block frequency Domain Adaptive Filter (see fig 4.1) [Ege]. The whitening is now done by multiplying the update operator $\underline{\nabla}$ with the inverse instantaneous power spectrum $\underline{P}^{-1}$, which is the Fourier transform of the inverse autocorrelation matrix R^{-1}.

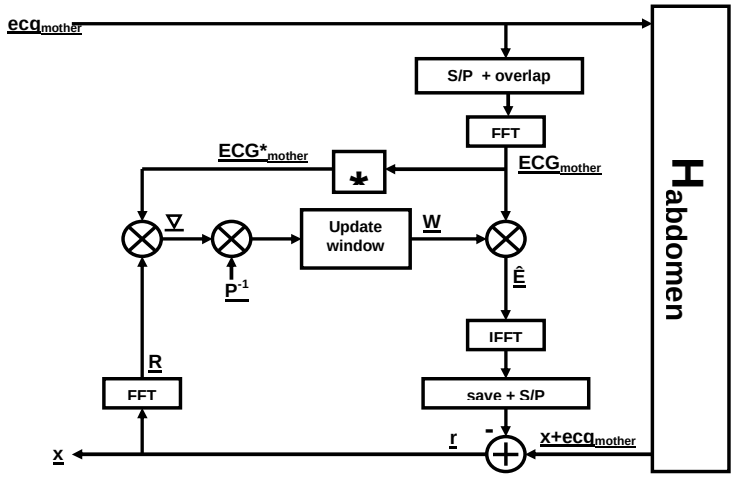

Figure 3.2: Block Frequency Domain Adaptive Filter (BFDAF)

3.1.3 Sample Rate Conversion

Because the EHG contains no information above 5 Hz and the measurments are sampled at 500 Hz, the recorded signal is downsampled to a samplerate of 10 Hz. This is done by first lowpass filtering the original signal and then decimating it. The low pass filtering is done with an Finite Impulse Response Filter in frequency domain; after transformating the EHG-signal to frequency domain (equation 3.14) by means of a DFT (the discrete version of the FT (equation 3.13)) the signal is multiplied with a rectangular window (equation 3.15).

$$X(j\omega) = \int_{-\infty}^{+\infty} x(t)e^{-j\omega t}dt \tag{3.13}$$

$$X[l] = \sum_{k=0}^{n-1} x[kT_1]e^{-\frac{2\pi j}{n}lk} \tag{3.14}$$

$$Y[l] = X[l]H[l] \tag{3.15}$$

with $H[l]$ the transferfunction of the filter, which is 1 at the frequency's that must be passed and 0 at frequency's that must be attenuated. After multiplying the signal is transformed back with the IDFT.

$$y[kT_1] = \frac{1}{n}\sum_{l=0}^{n-1} Y[l]e^{\frac{2\pi j}{n}lk} \tag{3.16}$$

The DFT and IDFT are implemented by a fast algorithm called the Fast Fourier Transform (FFT). The decimating is done by simply throwing samples away.

$$y[kT_2] = y[k(DT_1)] \tag{3.17}$$

with $D = \frac{T_2}{T_1}$ the decimation factor.

3.2 Determination of the Intra Uterine Pressure

3.2.1 Time-Frequency representation

The signal that is measured is not stationary. Therefore an ordinary Fourier Transform integrates all the FT components over the whole observation interval. A joint Time-Frequency distribution (TFD) is the solution to this problem. It gives a representation of the frequency's that are present at a certain moment in time. $\rho_z(t, f)$ is used as symbol for the TFD.

Noting that ρ_z is a function of frequency and represents a kind of spectrum, the FT of some function should be related to the TFD. This signal is called the signal kernel $K_z(t, \tau)$ and it's relation to the TFD is

$$\rho_z(t, f) = FT_{\tau \to f}\{K_z(t, \tau)\} \tag{3.18}$$

To find a suitable form for $K_z(t, \tau)$, the unit amplitude monocomponent FM signal is considered:

$$s(t) = e^{j\phi(t)} \tag{3.19}$$

whose instantaneous frequency is

$$f_i(t) = \frac{\phi'(t)}{2\pi} \tag{3.20}$$

The TFD of $s(t)$ should be a delta function at the instantaneous frequency:

$$\rho_z(t, f) = \delta(f - f_i(t)) \tag{3.21}$$

taking the IFT of equation 3.21 gives the signal kernel:

$$K_z(t, \tau) = e^{j\phi'(t)\tau} \tag{3.22}$$

Because $\phi'(t)$ is not directly available, it is substituted by

$$\phi'(t) = \lim_{\tau \to 0} \frac{\phi(t + \frac{\tau}{2}) - \phi(t - \frac{\tau}{2})}{\tau} \tag{3.23}$$

which can be approximated by

$$\phi'(t) = \frac{1}{\tau}[\phi(t + \frac{\tau}{2}) - \phi(t - \frac{\tau}{2})] \tag{3.24}$$

The signal kernel can now be written as

$$\begin{aligned} K_z(t, \tau) &= e^{j\phi(t+\frac{\tau}{2})} e^{-j\phi(t-\frac{\tau}{2})} \\ &= s(t + \frac{\tau}{2}) s^*(t - \frac{\tau}{2}) \end{aligned} \tag{3.25}$$

substituting 3.25 in 3.18 gives the so called Wigner distribution:

$$\begin{aligned} \rho_z(t, f) &= F_{\tau \to f}\{s(t + \frac{\tau}{2}) s^*(t - \frac{\tau}{2})\} \\ &= \int_{-\infty}^{+\infty} s(t + \frac{\tau}{2}) s^*(t - \frac{\tau}{2}) e^{-j2\pi f \tau} d\tau \end{aligned} \tag{3.26}$$

Equation 3.25 shows that the kernel is quadratic in the signal $s(t)$. Intuitively this is an reasonable assumption when the TFD is interpreted as a time-frequency energy distribution, since energy is a quadratic signal [Hla92]. An improvement of the Wigner Distribution is the Wigner Ville Distribution (WVD). The signal $s(t)$ is here replaced by it's analytic associated $z(t)$, removing all negative

frequency's that are normally present in a real signal. Doing this removes interactions of positive and negative frequencys in the TFD.

Other TFD's like the spectrogram are filtered versions of the WVD. This filtering is done by the double convolution (in time and frequency) of the WVD with a time frequency kernel $\gamma(t, f)$. Like in the fourier transform a convolution becomes a multiplication by a transformation to an other domain. This domain is called the ambiguity domain and the kernel is now referred to as Doppler-lag kernel $g(\nu, \tau)$ (see fig 3.3). The transformation to this domain is done by the (Fourier) transform from time to lag/ time shift ($t \rightarrow \tau$) and the transformation from frequency to Doppler/ frequency shift ($f \rightarrow \nu$) [Boa03].

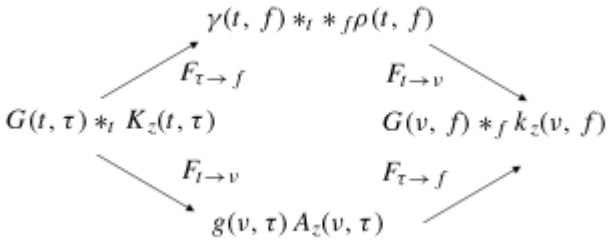

Figure 3.3: Domains and Transformations

For the spectrogram the Doppler-lag kernel is

$$g(\nu, \tau) = \int_{-\infty}^{+\infty} w(t + \frac{\tau}{2}) w(t - \frac{\tau}{2}) e^{-j2\pi\nu t} dt \tag{3.27}$$

with w the windowing function. The TFD os the spectrogram then becomes:

$$\rho_z(t, f) = \Big| \int_{-\infty}^{+\infty} z(\tau) w(\tau - t) e^{-j2\pi f \tau} d\tau \Big|^2 \tag{3.28}$$

To come to an optimal TFD, a Doppler-lag kern can be constructed that is dedicated to the signal. In this report, the WVD and spectrogram are considered.

3.2.2 Feature Extraction

Out of the TFD a representing feature has to be extracted that correlates with the real IUP. Earlier is mentioned that the EHG signal is an summation of frequency modulated signals (chapter 1.3). The instantaneous frequency of the EHG might give some information of the IUP. Because the measured signal is a filtered and summated version of different FM signals, no clear mono component signal can be expected to be in the TFD. Nevertheless a relevant feature with respect to frequency can be extracted, which is some average highest frequency, the mean instantaneous frequency:

$$\Omega(t) = \frac{\int_{-\infty}^{+\infty} f \rho(t, f) df}{\int_{-\infty}^{+\infty} \rho(t, f) df} \tag{3.29}$$

which is the first moment of the TFD in frequency.

Because of the temporal and spatial integration of FM signals, the amplitude of the signal also contains information of the IUP. By integrating the TFD w.r.t frequency the instantaneous power is

obtained:

$$p(t) = \int_{-\infty}^{+\infty} \rho(t, f) df \tag{3.30}$$

Multiplying equation 3.29 and 3.30 gives a new feature with both information about amplitude and frequency included:

$$\begin{aligned} \psi(t) &= \Omega(t) \cdot p(t) \\ &= \frac{\int_{-\infty}^{+\infty} f\rho(t, f) df}{\int_{-\infty}^{+\infty} \rho(t, f) df} \cdot \int_{-\infty}^{+\infty} \rho(t, f) df \\ &= \int_{-\infty}^{+\infty} f\rho(t, f) df \end{aligned} \tag{3.31}$$

3.2.3 Propagation of IUP

The propagation of IUP can give both information about the place of the pacemaker area and information about muscle fatigue. The propagation direction indicates where an contraction starts, while the speed of propagation is related with the fatigue of the uterus. The propagation is determined by the gradient of the delay (equation 3.32) between distinctive electrodes where the delay is calculated by the cross correlation between the electrode signal and the real IUP.

$$\underline{v} = -\nabla \underline{e}(x, y, \tau_{p\psi}) \tag{3.32}$$

where $\underline{e}(x, y, \tau_{p\psi})$ is a function that has a delay $\tau_{p\psi}$ at places (x, y). The minus sine in the equation comes from the fact that a more delayed signal started earlier in time. The delay $\tau_{p\psi}$ is found by taking the time where the cross correlation between the real and approximated IUP maximizes:

$$\tau_{p\psi} = \arg\max_{\tau} R_{p\psi}(\tau) \tag{3.33}$$

where the cross correlation $R_{xy}(\tau)$ is given by:

$$R_{xy}(\tau) = \begin{cases} \sum_{t=0}^{N-x-\tau} x(t+\tau)y(t) & \text{if } \tau \geq 0; \\ R^*_{xy}(-\tau) & \text{if } \tau < 0. \end{cases}$$

3.3 Post Processing

3.3.1 Multiple Regression

The relationship between the estimated IUP $\underline{\Psi}$ and the real IUP $\underline{Y}$ can be improved by calculating the real offset, gain and saturation. This can done by multiple linear regression, a method that estimates the conditional expected value of $\underline{Y}$ given the values of some other variables (equation 3.34), in this case some powers of $\underline{\Psi}$.

$$\underline{Y} = a + b\underline{\Psi} + c\underline{\Psi}^2 + d\underline{\Psi}^3 \tag{3.34}$$

where a models the offset, b the gain and d the saturation. The values of a, b, c and d are estimated by the method of least squares, that minimizes the sum of squares of the residuals:

$$\epsilon_r = \sum_{i=1}^{n} \left(y_i - (a + b\psi_i + c\psi_i^2 + d\psi_i^3 \right)^2 \tag{3.35}$$

By defining the matrix $\mathbf{X}$:

$$\mathbf{X} = \begin{bmatrix} 1 & \psi_1 & \psi_1^2 & \psi_1^3 \\ 1 & \psi_2 & \psi_2^2 & \psi_2^3 \\ \vdots & \vdots & \vdots & \vdots \\ 1 & \psi_n & \psi_n^2 & \psi_n^3 \end{bmatrix} \tag{3.36}$$

and parameter vector $\underline{P} = [a \quad b \quad c \quad d]$, the error ϵ_r can now be expressed as:

$$\epsilon_r(\underline{P}) = (\underline{Y} - \mathbf{X}\underline{P})^t(\underline{Y} - \mathbf{X}\underline{P}) = \underline{Y}^t\underline{Y} - 2\underline{P}^t\mathbf{X}^t\underline{Y} + \underline{P}^t\mathbf{X}^t\mathbf{X}\underline{P} \tag{3.37}$$

Normally the optimum is found by taking derivatives to $\underline{P}$ and set equal to zero. Another way to do this, not involving calculus is by taking the instantiation of $\underline{P}$, $\hat{\underline{P}}$ in such way that $\mathbf{X}^t\mathbf{X}\hat{\underline{P}} = \mathbf{X}^t\underline{Y}$ [Mis04]. Evaluating $\epsilon_r(\underline{P}) - \epsilon_r(\hat{\underline{P}})$:

$$\begin{aligned} \epsilon_r(\underline{P}) - \epsilon_r(\hat{\underline{P}}) &= \underline{P}^t\mathbf{X}^t\mathbf{X}\underline{P} - 2\underline{P}^t\mathbf{X}^t\underline{Y} + 2\hat{\underline{P}}^t\mathbf{X}^t\underline{Y} - \hat{\underline{P}}^t\mathbf{X}^t\mathbf{X}\hat{\underline{P}} \\ &= \underline{P}^t\mathbf{X}^t\mathbf{X}\underline{P} - 2\underline{P}^t\mathbf{X}^t\mathbf{X}\hat{\underline{P}} + \hat{\underline{P}}^t\mathbf{X}^t\mathbf{X}\hat{\underline{P}} \\ &= \left(\mathbf{X}(\underline{P} - \hat{\underline{P}})\right)^t\left(\mathbf{X}(\underline{P} - \hat{\underline{P}})\right) \end{aligned} \tag{3.38}$$

which is always greater than or equal 0, since it is a sum of squares. This implies:

$$\epsilon_r(\underline{P}) \geq \epsilon_r(\hat{\underline{P}}) \tag{3.39}$$

for all $\underline{P}$, which makes $\hat{\underline{P}}$ the optimum:

$$\hat{\underline{P}} = (\mathbf{X}^t\mathbf{X})^{-1}\mathbf{X}^t\underline{Y} \tag{3.40}$$

Calculating $\hat{\underline{P}}$ for many measurements can give information about the average $\hat{\underline{P}}$, which can be used for calculating the IUP, without measuring the real IUP.

Chapter 4

Results

Acquiring measurements is a difficult task because measurements with the pressure catheter can harm the baby or the mother. The kind of measurements needed for this study only are performed in case of medical necessity. Besides this lag of suitable patients there were some problems with the amplifier. Because of these problems only two measurements could be done. The results that are obtained are described in this chapter. Further the results are compared with another algortihm ([Vul05]. This algorithm has the same electrode configuration as done in this study. From these electrodes the best 4 electrodes are determined by independent component analysis (ICA). Hereafter from these 4 electrodes the spectrogram is determined whereafter the energy is calculated in the frequency band from 0.6 to 3 Hz. Further a threshold is applied to this energy function to determine if a burst is present.

4.1 Evaluating the results

The results that are obtained are compared with the IUP by calculating the correlation coefficient (R) and the signal to noise ratio (SNR):

$$R_{xy} = \frac{E\Big((X - \mu_X)(Y - \mu_Y)\Big)}{\sigma_X \sigma_Y} \tag{4.1}$$

This correlation coefficient is calculated sample base:

$$R_{xy} = \frac{\sum(x_i - \overline{x})(y_i - \overline{y})}{(n-1)\sigma_X \sigma_Y} \tag{4.2}$$

$$SNR = 10 \log_{10} \frac{\overline{Y}^2}{\overline{(Y - \Psi)}^2}; \tag{4.3}$$

The SNR is also calculated with the sample based mean.

4.2 Removing the mother ECG

Figure 4.1 shows the removal of the mother ECG. In the most lower picture the amount of mother ECG in the electrode signal is plotted. Clearly the adaptation can be seen; in the first seconds the weights have to converge, no ECG is detected yet. As the weights converge to the response of the abdomen, they match more with the ECG in the signal, giving a better subtraction of it.

In the final results, removing the mother ECG gives exactly the same results as don't doing this. Therefore it is not necessary to remove this ECG for approximating the IUP. In the results in the next paragraphs the mother ECG is not removed.

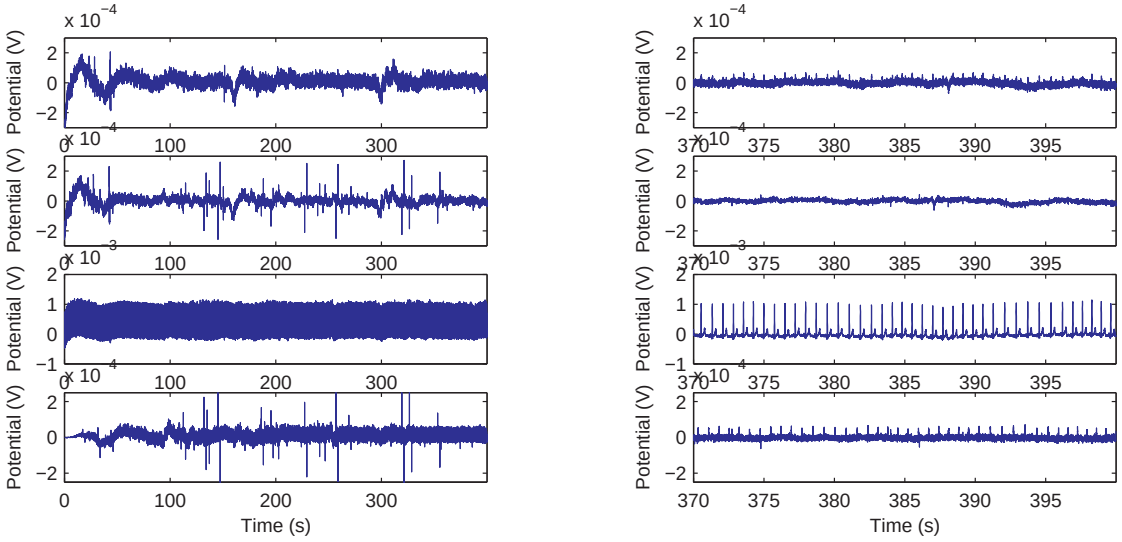

Figure 4.1: Block Frequency Domain Adaptive Filter (BFDAF) for removing the mother ECG: from up to down: the signal from the abdomen, the filtered signal, the mother ECG measured on the shoulder and the estimated ECG in the abdomen signal.

4.3 Time-Frequency representation

In figure 4.2 the Wigner Ville Spectrum and the spectrogram of a signal on the abdomen can be seen. The TFD of the spectrogram looks more smooth due to the filtering action of the window. The length for the time window is 40 seconds, which gives the highest correlation with the real IUP.

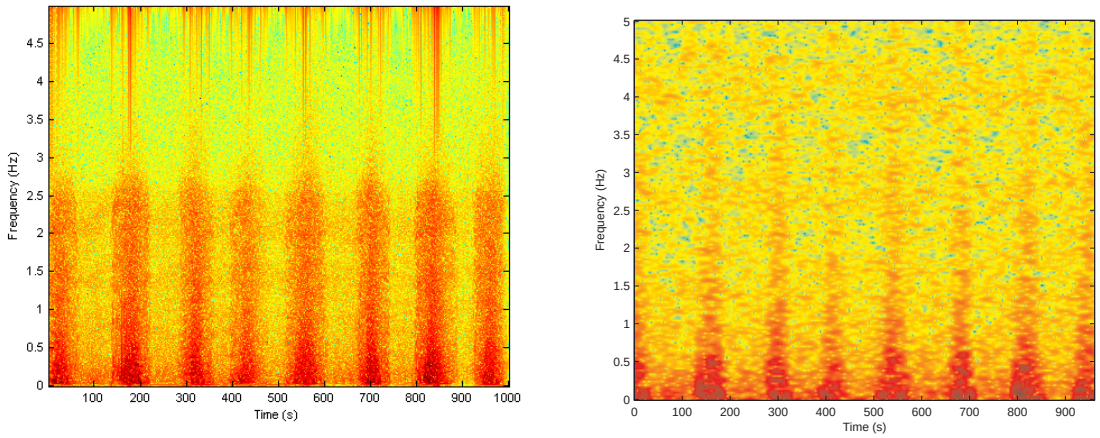

Figure 4.2: TFD: Wigner Ville (Left) and Spectrogram (Right)

4.4 The best frequency range

The best frequency range is determined by applying the algorithm to all possible frequency ranges from 0 to 5 Hz with a resolution of 0.1 Hz. The results (figure 4.3) point out that for the spectrogram two regions provide good results: frequency's from 0.2 to 1.1 Hz and frequency's from 3.4 to 3.6 Hz.

The spectrogram in figure 4.2 shows however that the lower band correlates the most with the real IUP. The Wigner Ville Spectrum performs well for almost all frequency ranges (figure 4.4), which makes this TFD more robust. The frequency range that performs best is from 0.7 to 2.4 Hz.

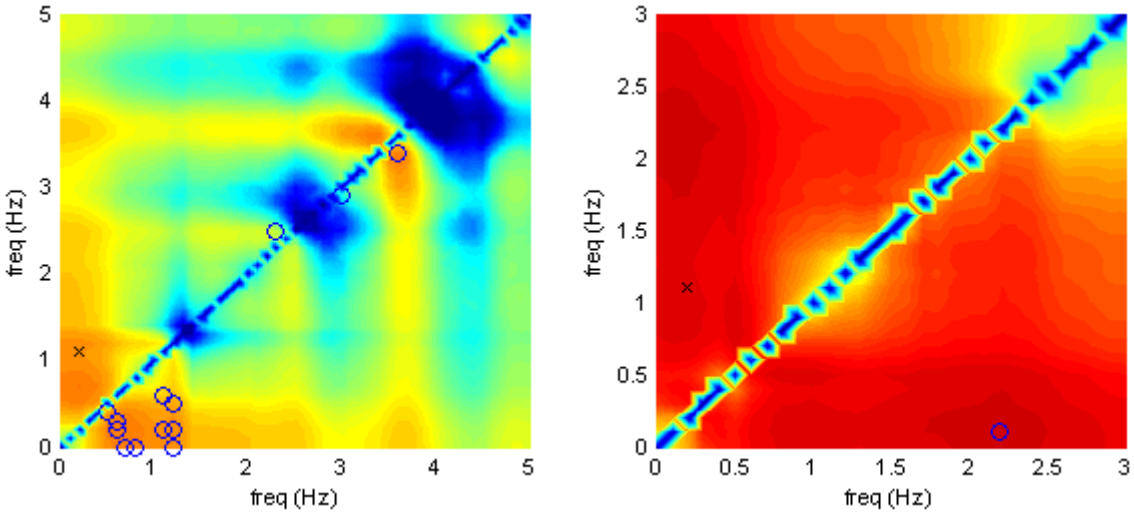

Figure 4.3: left: Frequency range of the average of all electrodes for patient 1 (spectrogram). right: Frequency range of bipolar lead 8 for patient 2 (spectrogram). The blue circles indicate the maximum that is found in de electrodes, the black cross the final chosen best frequency

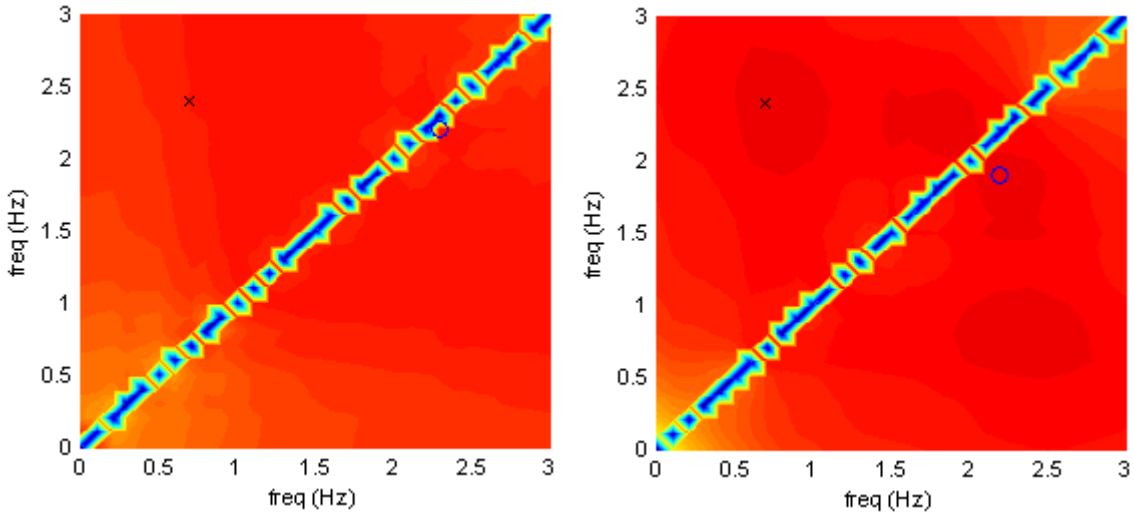

Figure 4.4: left: Frequency range of bipolar lead 8 for patient 1 (Wigner Ville). right: Frequency range of bipolar lead 8 for patient 2 (Wigner Ville). The blue circles indicate the maximum that is found in de electrodes, the black cross the final chosen best frequency

4.5 The best electrode position

From figure 4.5 can be seen that most electrodes have a high correlation with the real IUP. The bad results in the upper right corner of the uterus of patient 1 are most likely caused by a loose electrode.

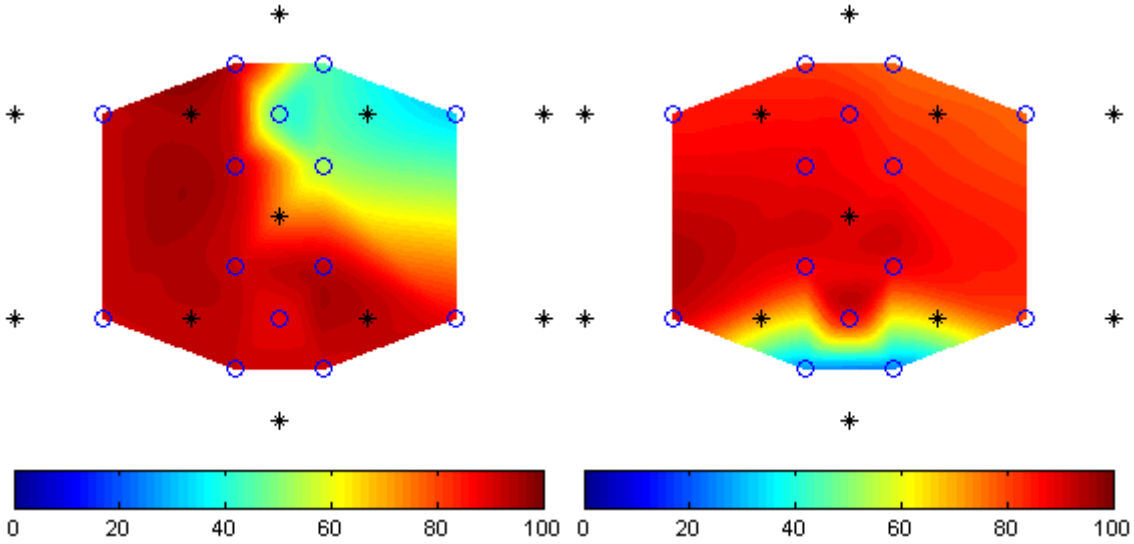

Figure 4.5: Correlation of the estimated and real IUP for different electrodes. Blue is no correlation, red is full correlation. Left: patient 1, Right: patient 2

Nevertheless, placing the electrodes somewhere at the middle of the abdomen is preferred because the tissue layer between uterus and abdomen is thinnest there. In this study electrodes somewhat below the middle of the abdomen (bipolar lead 8 and 9) give the best results. To specify the best measuring height the median line measurement was planned, which unfortunately couldn't be done. This measurement has a higher resolution in the length direction of the abdomen, which makes the determination of the best electrode position easier.

4.6 The approximated IUP

The final results are obtained by taking the mean of bipolar leads 8 and 9. Both spectrogram and Wigner Ville Spectrum are calculated with frequency ranges respectively from 0.2 - 1.1 Hz and from 0.7 - 2.4 Hz. The mother ECG is not removed for these measurements.

4.6.1 results for patient 1

In figure 4.6 the recording on the chest of the mother is shown. The quality of this signal is representive for all the electrodes. All segments of the ECG (P-top QRS-complex and T-top) can clearly be recognized in the signal indicating a good signal quality. The pressure catheter was not calibrated in this measurement which makes the values of the multiple regression of no value.

method	*correlation coefficient (p)*		*SNR*
Spectrogram	0.9657	(<0.001)	24.5677
Wigner Ville	0.9403	(<0.001)	24.9576
Other	0.7579	(<0.001)	0.3261

Table 4.1: Results for patient 1

In table 4.1 the results for patient 1 are shown. The spectrogram and Wigner Ville Spectrum both give a high correlation with the real IUP. The Wigner Ville Spectrum gives a better signal when there is no contraction, and is therefore preferred to use. The other algorithm gives worse results. This is most likely because the wrong frequency range is chosen and only the energy is taken as feature. Because

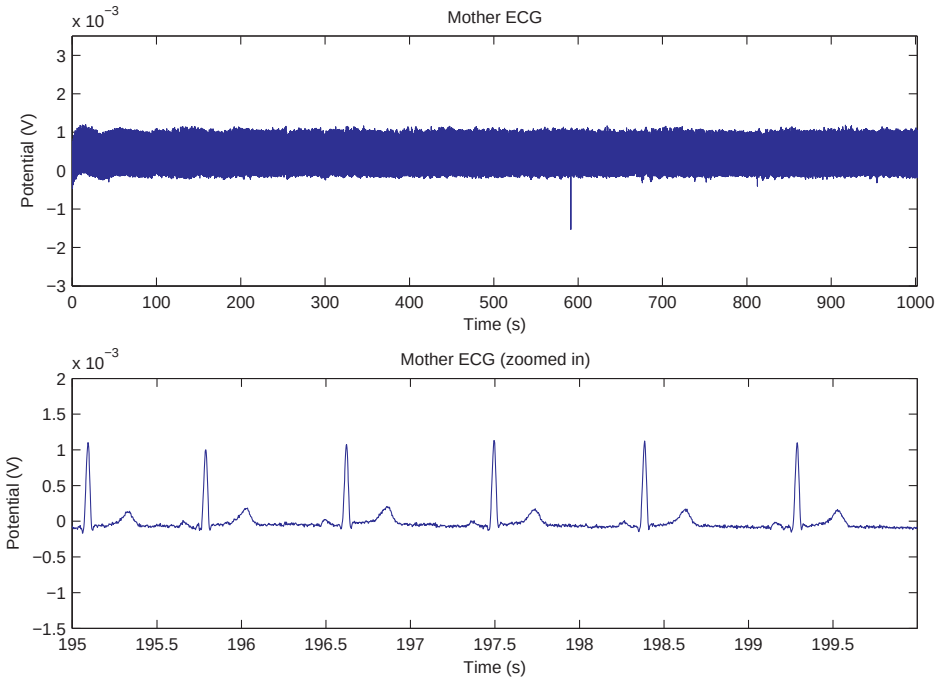

Figure 4.6: signal quality for patient 1. Top: the whole measurement. Down: zoomed in on a part.

of the ICA, this algorithm has also a much longer computation time than the algorithm developed in this study.

electrode	*mean (s)* $\pm$ *SD*	
1	27.5	0.9
2	26.4	16.5
3	28.5	0
4	24.9	17.8
5	27.1	12.1
6	26.4	0.3
7	30.5	11.6
8	26.9	0
9	25.8	0.2
10	29.8	1.3
11	27.5	2.0
12	27.2	0.1
13	26.5	1.1
14	27.1	0

Table 4.2: Mean delay's for all electrodes with their standard deviation for patient 1.

The propagation of contraction is calculated for each contraction. Table 4.2 shows that for patient 1 the calculated delay per contraction is consistent except for a few electrodes (2, 4, 5 and 7), which are just the electrodes with a bad estimated IUP (see figure 4.5). The contraction propagates through the whole uterus in about 5.5 seconds.

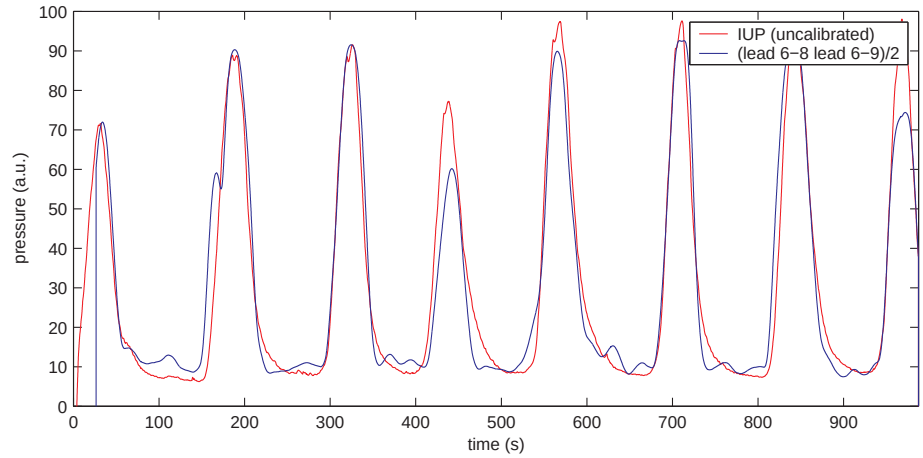

Figure 4.7: Estimated IUP for patient 1 with the spectrogram

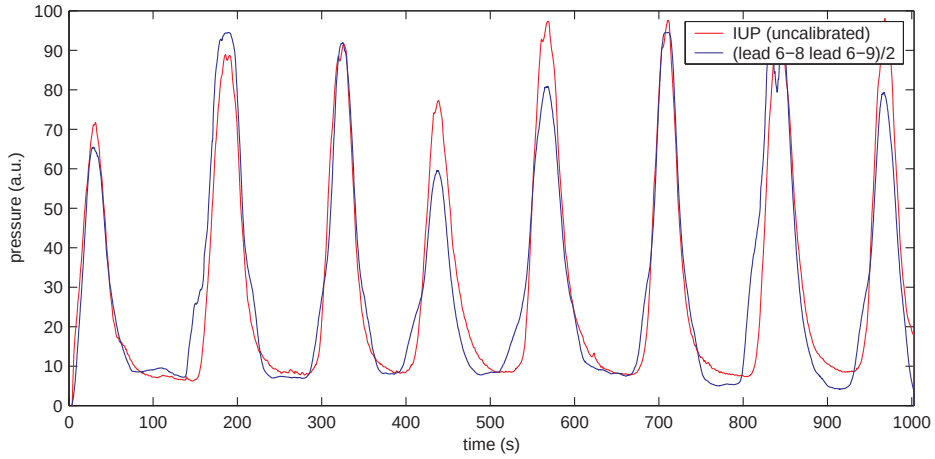

Figure 4.8: Estimated IUP for patient 1 with the Wigner Ville Spectrum

4.6.2 results for patient 2

In figure 4.11 the signalquality for patient 2 is plotted. In this case the signal is disturbed by motion artifacts, which can be seen on the while signal level as the spikes that are superimposed on the ECG. When zoomed in, the QRS-complex of the ECG can still be recognized. The P- and T-top of the ECG can't be recognized becose of the motion artifacts of people moving around the room. Further a 50 Hz component is still present in this signal.

method	*correlation coefficient (p)*		*SNR*
Spectrogram	0.9129	(<0.001)	10.5830
Wigner Ville	0.9172	(<0.001)	10.7803
Other	0.6238	(<0.001)	1.6409

Table 4.3: Results for patient 2

The results for patient 2 are qualitatively the same as for patient 1; the Wigner Ville Spectrum performs better because of the better signal when there is no contraction and the other algorithm performs worse than the ones proposed here.

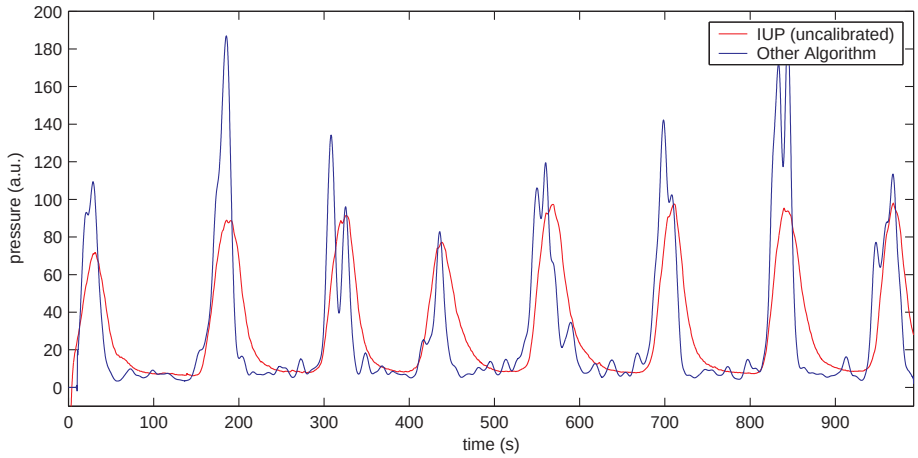

Figure 4.9: Estimated IUP for patient 1 with the other algorithm

electrode	*mean (s)* ± *SD*	
1	25.2	6.0
2	30.6	3.4
3	25.0	6.9
4	28.5	3.7
5	28.3	4.3
6	32.6	3.4
7	30.7	3.4
8	33.2	4.7
9	35.1	3.4
10	33.1	2.2
11	36.5	3.6
12	34.4	7.2
13	46.2	13.5
14	38.7	15.9

Table 4.4: Mean delay's for all electrodes with their standard deviation for patient 2.

For patient 2 holds the same as for patient 1, the calculated delay per contraction is consistent (see table 4.4) except for the electrodes that have a bad estimated IUP (13 and 14). The contraction propagates through the whole uterus in about 20 seconds.

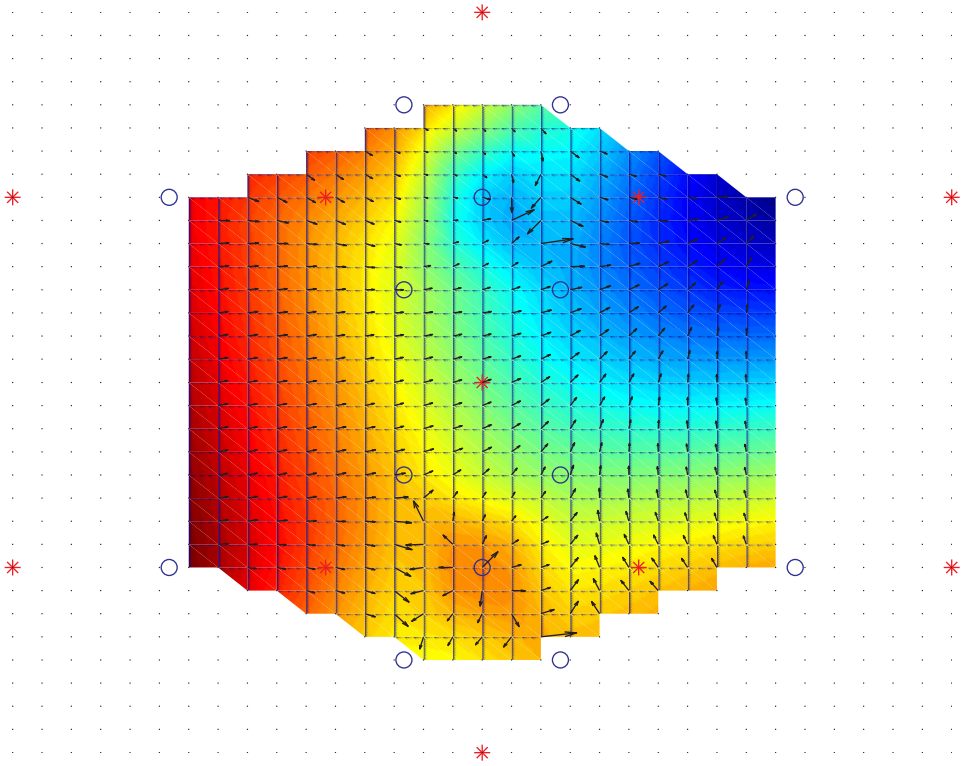

Figure 4.10: Propagation direction for patient 1

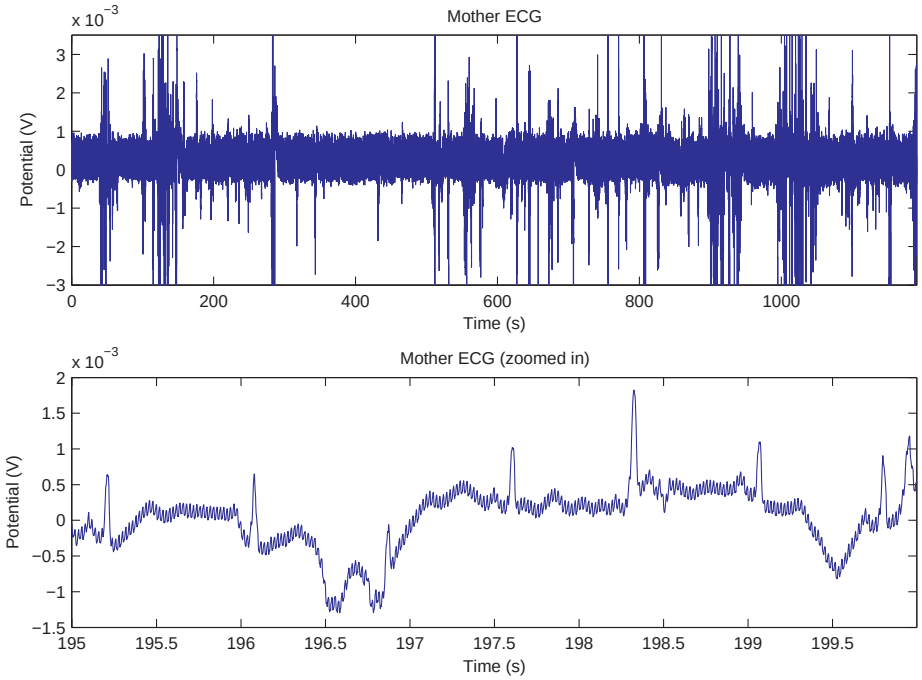

Figure 4.11: signal quality for patient 2. Top: the whole measurement. Down: zoomed in on a part

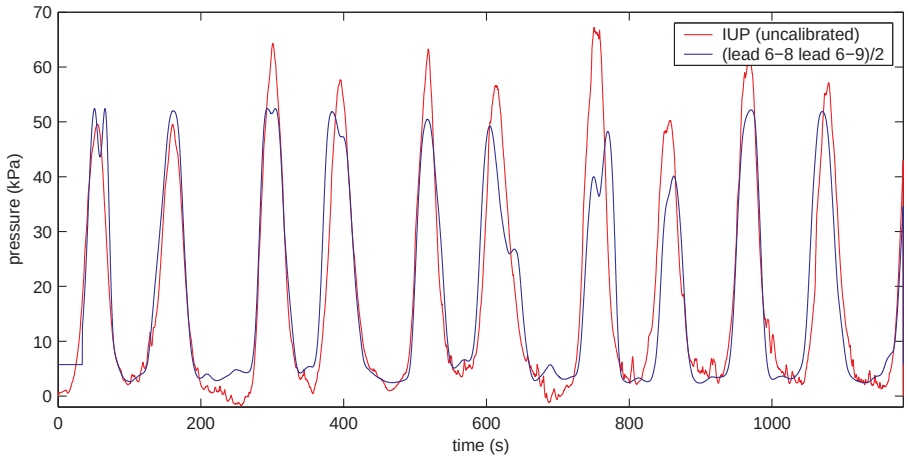

Figure 4.12: Estimated IUP for patient 2 with the spectrogram

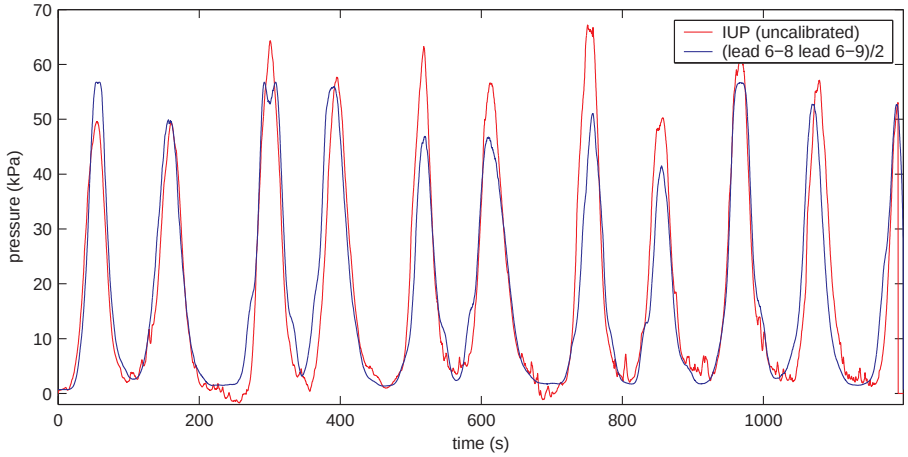

Figure 4.13: Estimated IUP for patient 2 with the Wigner Ville Spectrum

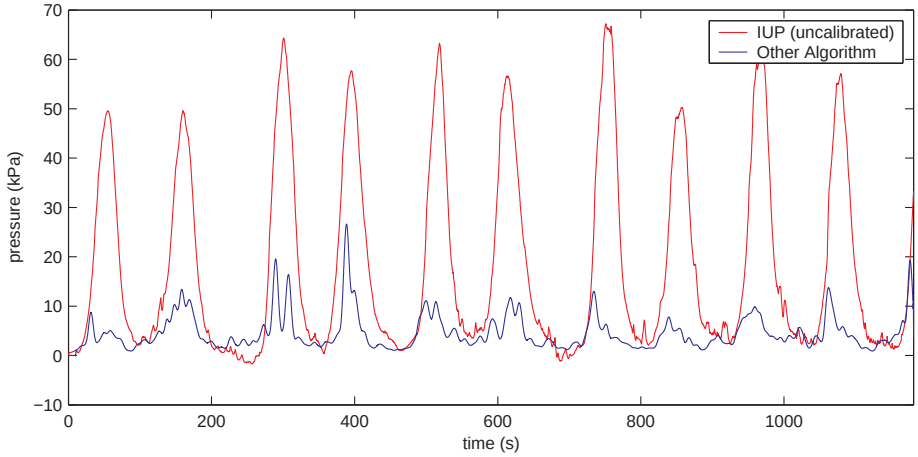

Figure 4.14: Estimated IUP for patient 2 with the other algorithm

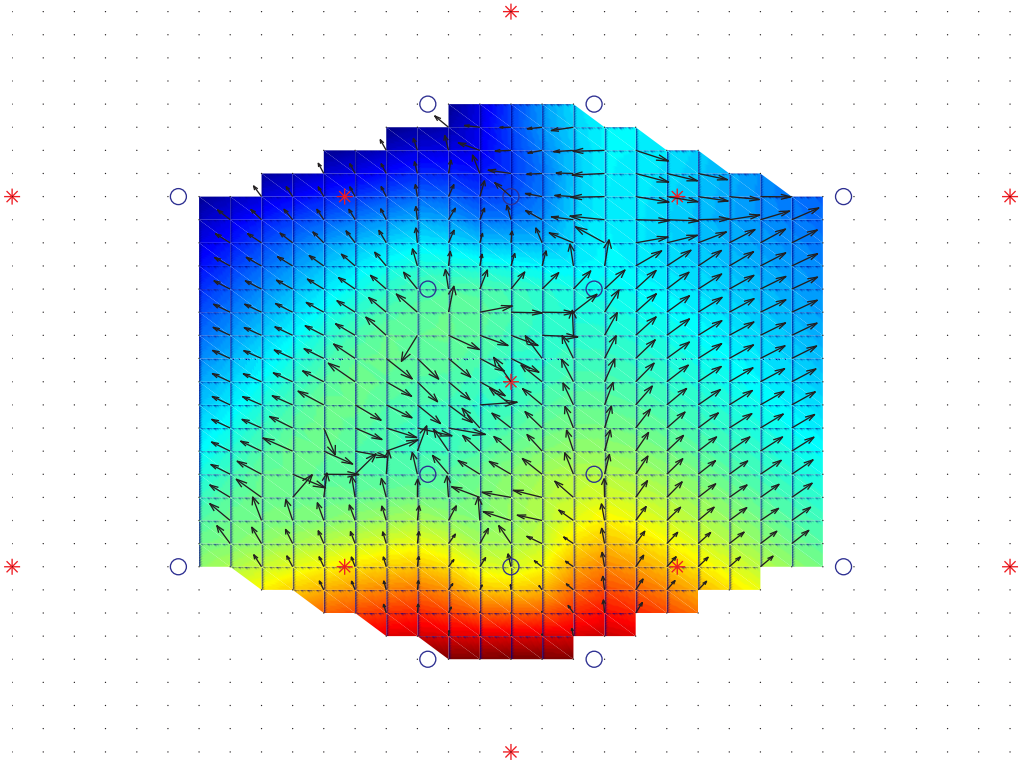

Figure 4.15: Propagation direction for patient 2

Chapter 5

Discussion

The electrodes that are used to perform the measurements are conventional AgCl unipolar electrodes. These electrodes average the electrical signals that comes from different places in the uterus. The solution for this might be the use of active Laplacian electrodes [Li05] which are capable of acquiring more localized information.

The algorithm that is developed, is not optimal because it is based on only two recordings. Acquiring measurements is a difficult task because measurements with the pressure catheter can harm the baby or the mother and are only performed in case of medical necessity.

Due to problems with the amplifier only one of the two available measurements is of good quality. The low quality measurement suffers from motion artifacts as people are moving around the room. Nevertheless the results for this measurement are comparable with the other recording.

Because of the two problems mentioned above, the measurement with the electrodes on a median line couldn't be performed which has as consequence that the best electrode position couldn't be determined accurately.

Further both recordings are performed during labour. For periods earlier in pregnancy the optimal frequency band can be different. This can be the case because stronger contractions are associated with a higher repetition of action potentials which indicates a frequency shift to higher frequency's.

The TFD's that are used in this report are the Wigner Ville Spectrum and the spectogram. A time-frequency kernel that is dedicated to the EHG likely gives better results.

Estimating the IUP with electrodes can be done with 2 or 3 electrodes on the abdomen. Determining the propagation direction and velocity however, is done with 12 electrodes which makes it an uncomfortable measurement for the women.

Chapter 6

Conclusion

In this study an algorithm is developed which calculates the IUP from 2 or 3 electrodes on the abdomen. Using 3 electrodes makes the algorithm more robust, because errors are averaged out. The intra uterine pressure can be measured on the whole surface of the abdomen that covers the uterus. A place somewhere in the middle is preferred because of the thinnest tissue layer there between the uterus and the abdomen. In this study electrodes somewhat below the middle of the abdomen (bipolar lead 8 and 9) give the best results.

After extracting the electrohysterogram out of the electrodes, the uterine pressure is determined out of a time frequency representation of the electrode signals. As TFD's the Wigner Ville Spectrum and spectrogram are used. Both TFD's give comparable results. However the Wigner Ville Spectrum is preffered because this TFD gives a smoother signal when there is no contraction. The TFD's give best results with a time window of +- 40 seconds.

From the TFD's can be seen that frequency's from DC to 3 Hz are present during a contraction. The best frequency range to calculate the IUP is determined in a brute force manner; simply compute all possible frequency ranges. The best frequency range for the Wigner Ville spectrum is 0.7 Hz - 2.4 Hz. For the spectrogram this range is 0.2 - 1.1 Hz.

The propagation of contractions is made visible which makes it possible to give additional information about muscle fatigue in the uterus muscle and information about contraction effectiveness.

The algorithm produces very good results with a correlation coefficient of over 90%. With this method it is possible to obtain the intra uterine pressure at an easy noninvasive manner, which makes it an alternative for tocography.

Bibliography

[Boa03] B. Boashash. *Time Frequency Signal Analysis and Processing: a Comprehensive Reference*. Elsevier, 2003.

[Clu98] P. Cluitmans. Elektrische metingen in de geneeskunde. 1998.

[Dev93] D. Devedeux. Uterine electromyography: A critical review. *Am J Obstet Gynecol*, 169(6):1636:1653, 1993.

[Ege] G. Egelmeers. A computationally efficient multi-channel block recursive least squares algorithm.

[Hla92] F. Hlawatsch. Linear and quadratic time-frequency signal representations. *IEEE SP Magazine*, page 21:67, April 1992.

[Hor01] K. Horoba. Algorithm for detection of uterine contractions from electrohysterogram. *IEEE EMBS Proc. Int. Conference*, page 2161:2164, October 2001.

[Li05] G. Li. Active laplacian electrode for the data-acquisition system of ehg. *Journal of Physics Conference Series*, 13:330:335, 2005.

[Man92] S. Mansour. Uterine emg spectral characteristics and instantaneous frequency measurement. *IEEE EMB Proc. Int. Conference*, 14:2602:2604, 1992.

[Man05] M.A. Mananas. Evaluation of muscle activity and fatigue in extensor forearm muscles during isometric contractions. *IEEE EMB Proc. Int. Conference*, September 2005.

[Mis04] M. Mischi. *Contrast echocardiography for cardiac quantifications*. PhD thesis, TU/e, 2004.

[Vul05] R. Vullings. The fetal electrocardiogram: Determination of the fetal heart rate and electrocardiogram from abdominal recordings. Master's thesis, TU/e, 2005.